5GPS: 5G Femtocell Placement Strategies for Ultra-Precise Indoor Localization in the Metaverse

Alireza Famili, Tolga O. Atalay, Angelos Stavrou
Department of Electrical and Computer Engineering, Virginia Tech, VA, USA
{afamili, tolgaoa, angelos}@vt.edu

***Abstract*—Mobile networks are rapidly evolving to cater to the expanding range of applications. The design of 5G deployments incorporates the concept of network slices, which are end-to-end logically isolated segments that provide distinct services. Within this delivery framework, augmented and virtual reality (AR/VR) wearables have gained prominence as a service type, thereby assuming a pivotal role in the realization of the Metaverse. Beyond the imperative need for stringent latency control, the successful implementation of the Metaverse relies significantly on the precise localization of user equipment (UE) within a three-dimensional (3D) environment. As the successor to the preceding 4G Long-Term Evolution (LTE), 5G networks operate at higher frequency ranges and denser deployment configurations. Within such dynamic contexts, ensuring high-precision indoor localization becomes a formidable challenge due to the unique signal characteristics associated with higher frequencies. In pursuit of this objective, we introduce the *5GPS* framework, which leverages established third-generation partnership project (3GPP) principles to conceptualize a radio access network (RAN) comprising 5G femtocells. This framework facilitates the offloading of positioning tasks from outdoor base stations (BSs) to enhance indoor positioning capabilities. The core contribution of our study lies in illustrating the pivotal impact of the spatial arrangement of 5G femtocells on the precision of positioning for AR/VR Metaverse wearable devices. To address this, we present a novel optimization framework for tackling the NP-Hard problem associated with femtocell deployment, thereby providing a comprehensive solution. We demonstrate that the utilization of our optimal placement solution results in a substantial enhancement in positioning accuracy when contrasted with arbitrary anchor deployments.**

***Index Terms*—indoor positioning, 5G, Metaverse, GDOP, optimal placement**

I. Introduction

The forthcoming mobile network evolution is anticipated to offer services across diverse sectors, each demanding distinct quality of service (QoS) standards. To accommodate this breadth of requirements, 5G and subsequent network generations rely on a heterogeneous radio access network (RAN). This RAN comprises 3rd Generation Partnership Project (3GPP) radio access technologies (RATs) to deliver wireless connectivity across a spectrum of environments.

Within this ecosystem, an emerging use case involves facilitating communication among Metaverse users. Companies such as Meta and Microsoft are striving to establish a seamless navigation infrastructure encompassing indoor/outdoor coverage for Metaverse users. As a result, the need for ultra-precise localization has become a foundational prerequisite.

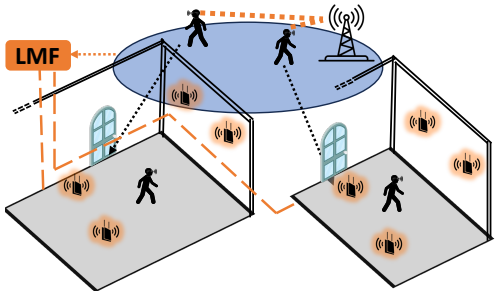

Figure 1: Overview of the 5GPS framework where localization is offloaded from the 5G base station to the 5G femtocell as the user moves indoors from outdoors

The Global Positioning System (GPS) is a renowned technology for delivering location data outdoors. However, it performs inadequately in enclosed indoor spaces, leading to service interruptions. While it is true that in legacy Long-Term Evolution (LTE) networks, the reported positioning accuracy is notably inferior to GPS, both cellular and GPS systems encounter challenges related to limited coverage within indoor settings.

The extensive deployment of heterogeneous 3GPP RANs in 5G has ushered in seamless communication capabilities for 5G-enabled Metaverse users, delivering dependable coverage and impressive throughput throughout their outdoor experiences. Nonetheless, the quest for a universal solution that guarantees highly accurate and reliable localization of Metaverse users across both indoor and outdoor environments remains an ongoing challenge. In response to this challenge and to provide strong coverage indoors, we propose the utilization of 5G femtocells for indoor localization. This approach enables Metaverse users to enjoy consistent and dependable localization throughout their entire engagement. A conceptual representation of this scenario is provided in Figure 1.

The positioning error within indoor environments exhibits a correlation with both ranging error and geometry-induced error. For instance, in a scenario where the ranging error is maintained at or below 10 cm, a benchmark achievable through the utilization of the ample bandwidth provided by 5G mm-Wave technology, the geometric dilution of precision (GDOP) for a specific location equates to 20. This consequently translates to a final localization error of around 2 m ($10\ cm \times 20 = 200\ cm$). This 20-fold increment from 10 cm to 2 m proves to be unsuitable for use cases where precise positioning is crucial.

Our primary objective is to investigate the implications of

979-8-3503-7099-7/24/$31.00 ©2024 IEEE

GDOP and optimize the placement of indoor anchors, which are referred to as positioning beacons, and are essentially 5G femtocells. While previous research in the literature [1]–[3] primarily concentrates on ameliorating ranging errors to enhance location accuracy, our approach encompasses considerations related to the system's spatial geometric configuration. Leveraging a novel optimization algorithm, we ascertain the most advantageous arrangement for 5G femtocells within a given indoor environment, thereby achieving high-precision positioning. To support this endeavor, we calculate the Cram'er-Rao Lower Bound (CRLB) on the position estimator, which elucidates that the localization error in time difference of arrival (TDOA) trilateration techniques is a consequence of both ranging inaccuracies and the relative geometric relationship between a user and positioning nodes.

Our experimental verification reveals that, even in scenarios marked by minimal ranging errors, the presence of poor GDOP can significantly impair the ultimate localization accuracy of Metaverse users within a three-dimensional (3D) space. Through the deployment of coverage heatmaps, we illustrate that GDOP stems from both vertical and horizontal dilution of precision (i.e., VDOP and HDOP), with the former exerting a more substantial influence on the overall degradation of estimation accuracy compared to the latter.

Our contributions are succinctly summarized as follows:

- The proposal of a comprehensive localization system integrating outdoor 5G base stations and indoor 5G femtocells, all seamlessly connected to a unified localization entity within the 5G core network.
- The establishment of an optimization framework utilizing Evolutionary Algorithms (EAs) to address the challenging NP-Hard problem associated with the placement of 5G femtocells within indoor settings.
- Conducting an analysis of the impacts of VDOP and HDOP to demonstrate that the former constitutes a more substantial error source in contrast to the latter. Consequently, this highlights the necessity for implementing more stringent constraints during the evaluation of the optimization problem.

II. 5GPS Core Network Model

In a 5G network, the uninterrupted retention of localization data is paramount, particularly for scenarios involving high-mobility User Equipment (UEs). Consequently, we introduce the model depicted in Fig. 2. This model establishes a unified core network repository for tracking the location details of a designated UE throughout its connection lifecycle in a heterogeneous 5G system with outdoor and indoor nodes.

The illustrated scenario presents both macro and micro base stations (BSs) designated for outdoor coverage via the 3GPP-standardized 5G NR [4]. Simultaneously, indoor coverage is achieved using 5G femtocells. A critical aspect of the connectivity lies in the conveyance of localization data, sourced both from outdoor 5G NR and indoor femtocells, to a singular Location Management Function (LMF) within the core network.

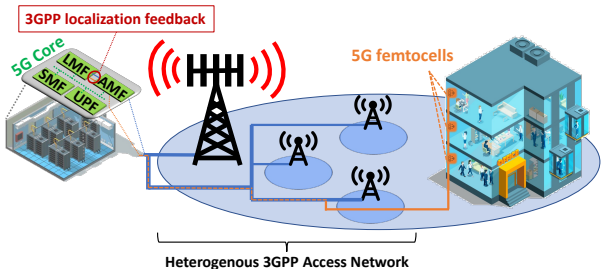

Figure 2: An overview of a multi-RAT 5G network with indoor/outdoor coverage and shared core network

This integration provides a comprehensive understanding of the drone's location within both the indoor and outdoor RANs.

In this configuration, the drone is capable of transitioning between outdoor nodes and indoor femtocells, ensuring the precision of its location is upheld in both external and internal environments. Moreover, this kind of hybrid deployment aligns with ongoing standardization endeavors. This alignment implies that there's no need to alter the LMF application programming interface (API).

In the subsequent sections of this paper, we delve further into the inaccuracies associated with indoor localization. We operate under the assumption of a stable outdoor cellular configuration, primarily consisting of 5G-NR nodes for positioning.

III. 5GPS Positioning

In this section, we commence with an overview of localization prerequisites. Subsequently, we explain how 5GPS ensures real-time, uninterrupted Metaverse user location data. Lastly, we determine the positioning error bound (PEB) and emphasize the critical role of spatial geometry in localization accuracy.

A. Fundamental Prerequisites for Localization

Our main focus centers on localization techniques rooted in ranging-based approaches [5]. These methods involve the utilization of signals transmitted and received between the user and anchor nodes. These signals can take the form of either acoustic [6] or Radio Frequency (RF) [7], depending on the type of transceivers employed. Beyond signal type, a localization system relies on an array of measurements, including Received Signal Strength (RSS), Time of Arrival (TOA), Time Difference of Arrival (TDOA), or Angle of Arrival (AOA).

Compared to RSS and AOA, a less complex yet highly reliable measurement method is TOA, which can be estimated without requiring extensive processing power or specialized antenna arrays [8]. Time measurements are translated into distance using the formula $r = c \times t$, where r represents the distance between the transmitter and receiver, c denotes the speed of the wave carrying the signal, and t signifies the time it takes for the waves to travel from the transmitter to the receiver. By obtaining distance measurements between multiple anchor nodes and the user, trilateration techniques can be employed to determine the final location.

A significant challenge associated with TOA techniques is the demand for precise synchronization between the user and

positioning nodes, a requirement often unattainable in practical settings. To that end, TDOA emerges as an alternative approach reliant on the measurement of arrival times without necessitating synchronization between users and positioning anchors.

B. 5GPS Trilateration

Within our setup, we depend on TDOA to enable 3D localization. In general, for the localization of an object in two dimensions via trilateration, a minimum of three anchor nodes are essential. Extending this to three dimensions, the requirement escalates to a minimum of four sources.

After successfully measuring the arrival time stamp at each of the 5G femtocells, trilateration based on the TDOA technique is executed to determine the user's 3D position.

Synchronization is not established between the Metaverse user and the 5G femtocells. Nonetheless, all the 5G femtocells possess synchronized clocks, facilitated by a wired connection among them. Consequently, the received times share the same synchronization bias, allowing for the representation of corresponding distances as follows:

$$r_i = c \times (t_i - t_T + \beta) = c \times (\tau_i + \beta), \tag{1}$$

where r_i denotes the corresponding distance between the Metaverse user and the i-th 5G femtocell, t_i is the received time at the i-th 5G femtocell, t_T is the transmit time, i.e., the time that the signal left the 5G transmitter on the Metaverse user, β is the synchronization bias between the user transmitter clock and any of the 5G femtocells, τ_i is the propagation time delay between the Metaverse user and the i-th 5G femtocell, and c is the speed of light; $i \in \{0, \cdots, N-1\}$, where N is the number of 5G femtocells which equals four in our design.

As evident in Eq. (1), the precise distances remain unknown due to the presence of the synchronization bias denoted by β. Nevertheless, the elimination of β becomes feasible when one of the anchors is regarded as the reference point as follows:

$$r_i - r_0 = c \times (t_i - t_0), \tag{2}$$

where $i \in \{1, \cdots, N-1\}$, and the precise measurement of t_0 and all the remaining t_i values exist. The geometric depiction of a set of points in a 3D space, where each point maintains a constant distance subtraction from three specified points (the foci), results in the formation of a hyperboloid. The intersection of these hyperboloids collectively denotes the user's location, expressed as follows:

$$[x \ y \ z]^T = \min \quad e(x, y, z), \tag{3}$$

where $[x \ y \ z]^T$ is the location of the user in a Cartesian coordinate system and $e(x, y, z)$ is defined as:

$$e(x, y, z) = \sum_{i=1}^{N-1} \left\{ (r_i - r_0) - \sqrt{(x_i - x_0)^2 + (y_i - y_0)^2 + (z_i - z_0)^2} \right\},$$

where $[x_i \ y_i \ z_i]^T$ values are the Cartesian coordinates of the $i-$th 5G femtocell.

C. 5GPS Positioning Error Bound

A valuable metric for evaluating localization precision is the Cramer Rao Lower Bound (CRLB), representing the minimum achievable location variance when utilizing an unbiased location estimator. Assuming independence and a zero-mean Gaussian noise with constant variance σ_r^2 in range measurements [9], the positioning error bound for 5GPS is derived.

As previously mentioned, obtaining an accurate estimation of r_i is not feasible. Nevertheless, precise clock synchronization among the 5G Femtocells facilitates the accurate calculation of the difference $r_i - r_j$. To proceed with the remaining steps, we designate r_0 as the reference femtocell and compute the values of $r_i - r_0$ as follows:

$$\begin{aligned} r_i - r_0 = &\sqrt{(x - x_i)^2 + (y - y_i)^2 + (z - z_i)^2} \\ &- \sqrt{(x - x_0)^2 + (y - y_0)^2 + (z - z_0)^2}. \end{aligned} \tag{4}$$

Due to the presence of ranging measurement inaccuracies, the precise value of $r_i - r_0$ remains unknown, leading to errors when solving for $[x \ y \ z]^T$ in Equation (4). In order to establish a relationship between the collective 3D positioning error, denoted as $\sigma_T(x, y, z)$, and the distance estimation errors, σ_{r_i}, originating from the measurement devices, it is essential to determine the variance of the 3D location estimator:

$$\sigma_T(x, y, z) = \sqrt{\sigma_x^2 + \sigma_y^2 + \sigma_z^2}, \tag{5}$$

where $(\sigma_x^2, \sigma_y^2, \sigma_z^2)$ are the variances of the error for $x-$, $y-$, and $z-$axis estimation, respectively. Let $\mathbf{\Delta X} = [\Delta x \ \Delta y \ \Delta z]^T$ be the derivative on the $[x \ y \ z]^T$ estimations; then, for the positioning variance, based on Eq. (5), we have:

$$\sigma_T^2(x, y, z) = \mathbf{Trace}\left(\mathbf{E}\left(\mathbf{\Delta X \Delta X^T}\right)\right), \tag{6}$$

and $\mathbf{Trace}(.)$ denotes the sum of the diagonal elements of the matrix. Next, the correlation between $\sigma_T^2(x, y, z)$ and the $\sigma_{r_i}^2$ is derived. To achieve this, we differentiate Eq. (4), that is

$$\begin{aligned} \Delta r_i - \Delta r_0 = &\frac{\Delta x(x - x_i) + \Delta y(y - y_i) + \Delta z(z - z_i)}{\sqrt{(x - x_i)^2 + (y - y_i)^2 + (z - z_i)^2}} \\ &- \frac{\Delta x(x - x_0) + \Delta y(y - y_0) + \Delta z(z - z_0)}{\sqrt{(x - x_0)^2 + (y - y_0)^2 + (z - z_0)^2}}, \end{aligned} \tag{7}$$

where second- and higher-order terms have been neglected. For the localization system with N 5G femtocells, Eq. (7) can be written as $\mathbf{\Delta R_i - \Delta R_0 = \Psi \Delta X}$, or equivalently $\mathbf{\Delta X} = (\mathbf{\Psi}^T \mathbf{\Psi})^{-1} \mathbf{\Psi}^T (\mathbf{\Delta R_i - \Delta R_0})$; where $\mathbf{\Delta R_i} = [\Delta r_1 \ \cdots \ \Delta r_{N-1}]^T$, $\mathbf{\Delta R_0} = [\mathbf{\Delta r_0} \ \cdots \ \mathbf{\Delta r_0}]^\mathbf{T}$, and

$$\mathbf{\Psi} = \begin{bmatrix} \frac{x - x_1}{r_1} - \frac{x - x_0}{r_0} & \frac{y - y_1}{r_1} - \frac{y - y_0}{r_0} & \frac{z - z_1}{r_1} - \frac{z - z_0}{r_0} \\ \vdots & \vdots & \vdots \\ \frac{x - x_{N-1}}{r_{N-1}} - \frac{x - x_0}{r_0} & \frac{y - y_{N-1}}{r_{N-1}} - \frac{y - y_0}{r_0} & \frac{z - z_{N-1}}{r_{N-1}} - \frac{z - z_0}{r_0} \end{bmatrix}.$$

We can make the assumption, without loss of generality, that Var(r_i) = σ_r^2, and that the errors Δr_i are uncorrelated. Thus:

$$\mathbf{Cov}(\mathbf{\Delta X}) = \mathbf{\Phi}\left(\mathbb{I}_{\mathbf{N-1}} + \mathbb{J}_{\mathbf{N-1}}\right)\mathbf{\Phi}^T \sigma_r^2, \tag{8}$$

where $\mathbf{\Phi} = (\mathbf{\Psi}^T \mathbf{\Psi})^{-1} \mathbf{\Psi}^T$, $\mathbb{I}_{\mathbf{N-1}}$ is the identity matrix of size

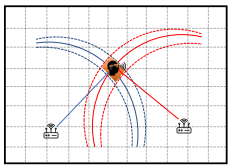

(a) Beacon placement with low location estimation error

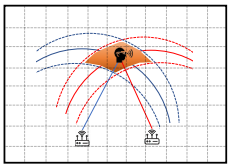

(b) Anchor placement with high location estimation error

Figure 3: Comparison of GDOP on location estimation error due to different anchor placement

Table I: Evaluation of GDOP Values

GDOP Values	Evaluation of the Geometry
1	Ideal
$1-2$	Very Good
$2-5$	Good
$5-10$	Medium
$10-20$	Sufficient
>20	Bad

$(N-1)\times(N-1)$ and $\mathbb{J}_{\mathbf{N-1}}$ is the $(N-1)\times(N-1)$ matrix with all its entries equal to one. Based on Eq. (6) the variance of the 3D location estimator is:

$$\sigma_T^2(x,y,z) = G(x,y,z)\cdot\sigma_r^2, \tag{9}$$

and $G(x,y,z) = \mathbf{Trace}\left(\mathbf{\Phi}(\mathbb{I}_{\mathbf{N-1}}+\mathbb{J}_{\mathbf{N-1}})\mathbf{\Phi}^T\right)$.

As a result, the overall location accuracy is influenced by the geometry-induced error $G(x,y,z)$, which is entirely determined by the relative geometry between the localization anchors and the user.

In satellite navigation $G(x,y,z)$ is known as GDOP which is a term used to specify the error propagation as a mathematical effect of navigation satellite geometry on positional measurement precision.

GDOP consists of HDOP and VDOP, $GDOP = \sqrt{HDOP^2+VDOP^2}$. HDOP, which is the $G(x,y)$, represents the effect of the relative geometry between positioning anchors and the user on the $X-Y$ plane, while VDOP, $G(z)$, shows the impact of geometry on the Z-axis estimation. Table I shows the evaluation of the GDOP values.

The graphical representation of GDOP is presented in Fig. 3 for two distinct scenarios. In the first scenario, illustrated in Fig. 3a, the beacons exhibit a more favorable placement in comparison to the configuration shown in Fig. 3b. Consequently, this disparity leads to varying location estimation errors, as evident in the respective shaded regions.

We aim for optimal GDOP while ensuring reasonably low HDOP and VDOP values simultaneously. Good HDOP with poor VDOP results in accurate 2D localization but poor Z-axis estimation. Most existing literature focuses on 2D localization [9], [10], which is why they often overlook optimal anchor deployment. Yet, in 3D environments like the Metaverse, precise Z-axis estimations are crucial. In this section, we introduced GDOP, HDOP, and VDOP to address localization errors. In the next section, we propose an algorithm for optimal 5G femtocell placement in indoor settings to achieve favorable GDOP, HDOP, and VDOP.

IV. 5GPS Femtocell Deployment Strategy

Recent years have witnessed extensive research into anchor placement optimization, addressing both indoor localization [9]–[13] and wireless network configurations [14], [15]. This research primarily focuses on determining the optimal number of anchors necessary to effectively cover a given indoor space, which is heavily influenced by the sensor technology in use, given the diverse coverage capabilities they offer. For instance, in low-power Bluetooth systems, the transmission is typically omnidirectional whereas ultrasound-based systems have beam angle constraints, impacting sensor quantity and placement [16].

Previous localization methodologies primarily focused on stationary targets within 2D scenarios, thus neglecting the intricate spatial relationships that exist in three dimensions between the target and anchor points. Consequently, determining the optimal placement for a mobile target within a 3D space remains an ongoing challenge [10]. Furthermore, establishing an anchor placement configuration for indoor localization that minimizes the relative geometric error between the nodes of the localization system and the user at any given position has been recognized as a well-established NP-Hard problem [9]–[12].

In this section, we introduce an optimization algorithm designed to determine the optimal placement of 5G femtocells with the aim of reducing the localization error resulting from unfavorable relative geometry. The presented optimization algorithm is devised to ensure that both the $X-Y$ plane (horizontal) and the Z-axis (vertical) exhibit high levels of accuracy in localization estimation.

It is worth noting that the Z-axis is especially susceptible to errors from geometric factors. Even when the overall GDOP for a given point is favorable, there is no guarantee that the VDOP will be as favorable as the HDOP for the same point. This often leads to precise estimations in the $X-Y$ plane but substantial inaccuracies in the Z-axis estimations.

To the best of our knowledge, we are the first to propose an algorithm aimed at enhancing the localization accuracy for indoor Metaverse users, encompassing both the $X-Y$ plane and the Z-axis.

To tackle the NP-Hard problem, we employ two constraints related to the average values of $G(x,y)$ and $G(z)$. Once these constraints are met, the configuration with the lowest $G(x,y,z)$ value represents the final solution. Although there might be other solutions with similar or lower $G(x,y,z)$ values, our primary objective is to ensure that the location estimation for every point in the room is minimally affected by the relative placement of anchors. Therefore, finding a configuration that meets the specified thresholds for the averages of $G(x,y)$ and $G(z)$ fulfills our goal. This approach streamlines our optimization algorithm while preserving our commitment to minimizing the impact of geometric factors.

In the remainder of this section, we explain the details of our proposed optimization framework. In Sec. IV-A, we

formulate the NP-Hard optimal placement problem followed by the illustration of the optimization algorithm's mechanism in Sec. IV-B.

A. Problem Formulation

Considering the continuous mobility of the user, the computation of $G(x, y, z)$, $G(x, y)$, and $G(z)$ for a single location is insufficient. Therefore, we calculate their averages across all points within the indoor space, based on the provided floor plan. Our objective is to identify the optimal placement for a set of four 5G femtocells by minimizing the average value of $G(x, y, z)$, denoted as $\overline{G(x, y, z)}$, while ensuring that the averages of $G(x, y)$ and $G(z)$, represented as $\overline{G(x, y)}$ and $\overline{G(z)}$ respectively, remain below the specified threshold levels. The ultimate optimization can be expressed as follows:

$$\begin{aligned} \min \quad & \textstyle\sum_{\mathbb{U}} \mathbf{Trace}\left(\mathbf{\Phi}(\mathbb{I}_{\mathbf{N-1}} + \mathbb{J}_{\mathbf{N-1}})\mathbf{\Phi}^T\right) \\ s.t. \quad & \overline{G(x, y)} < h_T;\ \overline{G(z)} < v_T \end{aligned}$$

where $\mathbb{U}$ is the user domain which is a subspace of the indoor environment that includes all the possible positions where the Metaverse user can be, $\mathbf{\Phi}$ comes from Eq. (9), h_T, and v_T are the threshold values for $\overline{G(x, y)}$ and $\overline{G(z)}$, respectively.

Our objective is to minimize $\overline{G(x, y, z)}$ with the aim of enhancing localization accuracy. Simultaneously, we enforce constraints on $\overline{G(x, y)}$ and $\overline{G(z)}$ to maintain low horizontal and vertical estimation errors. This approach guarantees that overall localization accuracy improvement encompasses both the estimation of the $X - Y$ plane and the Z-axis. These computations are extended across all points within the set $\mathbb{U}$.

The anchor domain, denoted as set $\mathbb{A}$, encompasses the permissible region for the deployment of 5G femtocells. It includes the entirety of the ceiling and the upper half portion of all the side walls.

B. Placement Framework

In order to minimize computational time, we have designed a program utilizing the evolutionary algorithms (EAs) class. Initially, within our evolutionary algorithm (EA) framework, we generate a set of P_T random individuals. Each individual is comprised of four 5G femtocells, chosen at random from the domain $\mathbb{A}$. To mitigate the risk of converging into local minima, these individuals are distributed into distinct groups.

Algorithm 1 5G Femtocells Deployment Algorithm

Input: User domain ($\mathbb{U}$), Anchor domain ($\mathbb{A}$), $\overline{G(x, y)}$ threshold (h_T), $\overline{G(z)}$ threshold (v_T)
Output: Placement of a set of four 5G femtocells

```
while Ḡ(z) > v_T & Ḡ(x,y) > h_T do
    Generate a set of P_T random individuals, where each individual is a set of four 5G femtocell anchors
    for i = 1 to i = number of iteration do
        Check the fitness of all available individuals;
        Kill the worst ones to keep having P_T individuals;
        Select the individuals with better fitness as parents;
        Crossover adjacent parents, make an offspring;
    end for
end while
```

Table II: 5G femtocells placement for different room sizes with a random solution to benchmark the optimal case

Room Dimensions	5G-FC #1	5G-FC #2	5G-FC #3	5G-FC #4
Office Room (5m × 5m × 4m)	(3,4,4)	(3,2,4)	(3,1,4)	(4,1,4)
Conference Room (10m × 10m × 4m)	(6,10,4)	(2,7,4)	(3,7,4)	(7,1,4)
Game Room (20m × 20m × 4m)	(18,10,4)	(14,3,4)	(19,11,4)	(14,1,4)

Following the initial generation, the individuals are arranged in accordance with their fitness (cost) function, and the selection for reproduction is based on the obtained results. The fitness function, which is the average of $G(x, y, z)$ over the complete set $\mathbb{U}$ using a specific configuration of four 5G femtocells, serves as the criterion. Subsequently, the algorithm chooses the first P_s individuals as the parent group to create new offspring.

Each pair of adjacent individuals in the parent group participates in a crossover process, yielding a total of $P_s/2$ offspring. The algorithm then reevaluates the fitness function for each new individual. From the total population of $P_n = P_T + P_s/2$, the least fit $P_k = P_s/2$ individuals are removed, resulting in a final population of P_T individuals.

In the process of generating new offspring, each set of parents comprises a total of eight 5G femtocells, with four belonging to each parent. The crossover technique involves interchanging the coordinate parameters of the first four 5G femtocells with those of the second set.

Once the specified number of iterations, denoted as N_{iter}, ends, the first individual in the lineup, determined by the fitness function, is chosen. If this individual exhibits an $\overline{G(x, y)}$ and $\overline{G(z)}$ below the respective thresholds of h_T and v_T, then this individual serves as the definitive solution, representing the configuration for the placement of the four 5G femtocells.

In cases where the selected individual does not meet these criteria, the algorithm restarts by generating a fresh batch of P_T individuals and reinitiating the procedure. The algorithm continues this iterative process until a result is obtained that complies with the specified constraints.

The values for P_T, P_s, and N_{iter} are established during the pre-processing phase, a critical step that factors in the specifics of the given floor plan. The selection of these parameters involves careful consideration and may necessitate a trade-off between computational efficiency and the precision of the solution. It is worth noting that the flexibility in adjusting parameters allows for adaptability to various floor plans, thereby enhancing the overall utility of this approach in addressing geometric-induced localization errors.

V. Results & Evaluations

Within this section, our presentation unfolds in two phases. Initially, we present the outcomes arising from the arbitrary

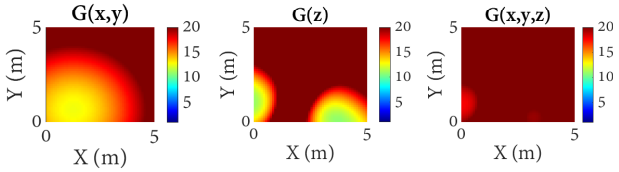

(a) Random configuration for an office room

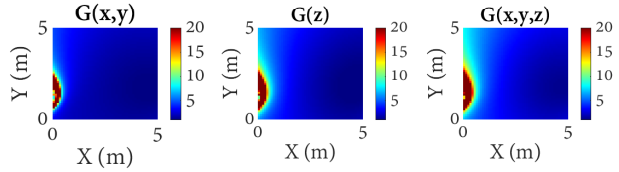

(b) Optimal configuration for an office room

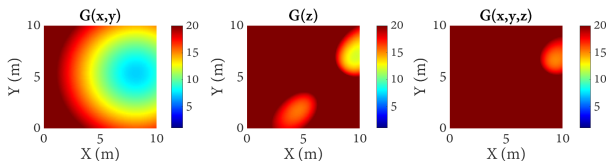

(c) Random configuration for a conference room

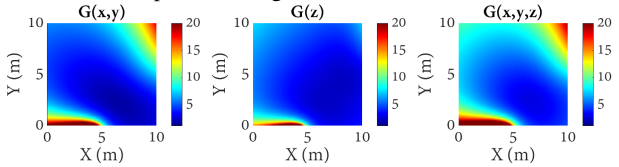

(d) Optimal configuration for a conference room

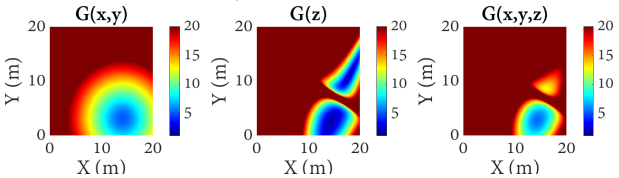

(e) Random configuration for a game room

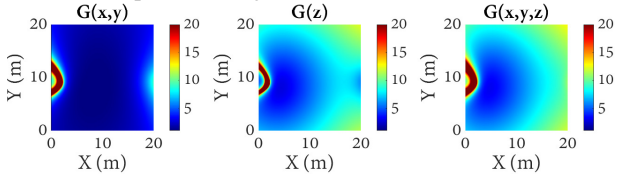

(f) Optimal configuration for a game room

Figure 4: Comparison of $G(.)$ Values: Random vs. Optimal Placement in Varied Indoor Space Dimensions

Table III: 5G femtocells placement for different room sizes with optimal solution

Room Dimensions	5G-FC #1	5G-FC #2	5G-FC #3	5G-FC #4
Office Room (5m × 5m × 4m)	(0,1,2)	(5,1,2)	(5,5,3)	(2,2,4)
Conference Room (10m × 10m × 4m)	(7,3,4)	(6,1,4)	(0,9,4)	(8,0,2)
Game Room (20m × 20m × 4m)	(19,10,4)	(3,8,4)	(8,20,3)	(2,0,2)

placement of anchors. This is done to underscore the pronounced influence of geometric considerations on both the GDOP and the ultimate accuracy of positioning. Subsequently, we transition to a comprehensive exposition of the results stemming from the implementation of our deployment framework to assess the performance of our proposed algorithm.

The simulations were conducted using *MATLAB 2022a* on a *Dell Optiplex 7080* computer. Simulations are based on the deployment of four 5G femtocells. The primary goal of these simulations is to determine the optimal arrangement of these femtocells, a configuration that is inherently dependent on the dimensions of the room, specifically the provided floor plan. Accordingly, our algorithm takes the floor plan as input and furnishes the optimal placement for the 5G femtocells as output.

To assess the algorithm's effectiveness and adaptability, it has been tested on three distinct floor plans, each representing different room dimensions. The first scenario involves a typical office room with dimensions of $5\ m \times 5\ m \times 4\ m$, designed for virtual gaming experiences using virtual reality (VR) devices. The second scenario encompasses a larger space, a conference room measuring $10\ m \times 10\ m \times 4\ m$, suitable for augmented reality (AR) applications in more expansive settings. Lastly, the algorithm is put to the test in an extreme scenario, a large game room spanning $20\ m \times 20\ m \times 4\ m$, catering to multi-user AR/VR games such as laser tag. These diverse tests showcase the algorithm's versatility across room dimensions ranging from moderate to exceedingly spacious.

The proposed algorithm is anticipated to exhibit favorable performance, especially in scenarios with smaller room dimensions. Impressively, it has demonstrated its capability to efficiently generate optimal solutions even for substantially larger spaces. Moreover, in instances where the dimensions are exceedingly large, such as a room measuring $100\ m \times 100m \times 4\ m$, where the coverage range of 5G femtocells may fall short of spanning the entire floor plan, the sole adjustment needed is the introduction of additional 5G femtocells to meet the coverage demands.

The non-optimized benchmark and the optimal deployments are enumerated in Table II and Table III, respectively. The measurements in both tables are presented in meters.

Our objective is to illustrate the xDOP values, encompassing HDOP, VDOP, and GDOP, which are represented as $G(.)$ values, namely $G(x, y)$, $G(z)$, and $G(x, y, z)$, within 3D spaces. To achieve this, we compute the average xDOP values for each (x, y) point across all z planes and present them through heat maps. This approach not only simplifies the spatial representation but also allows us to consider all z planes comprehensively, as opposed to just a limited subset, leading to more inclusive results.

In order to discern the distinct impacts on localization accuracy between the $X-Y$ plane and the Z-axis, we depict HDOP, VDOP, and GDOP individually. This enables us to highlight scenarios where a particular configuration may yield favorable horizontal accuracy but less satisfactory vertical estimations, thereby providing a more nuanced view of the performance.

Figure 4 illustrates a comparative analysis of xDOP values, examining both optimal and random placements. The displayed

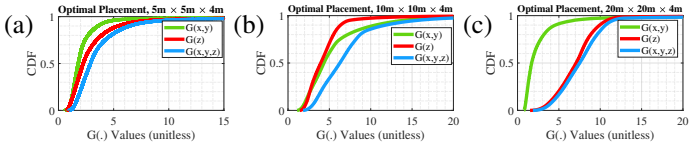

Figure 5: CDF plot representation of $G(.)$ values for various room dimensions with optimal configuration shown in Table III

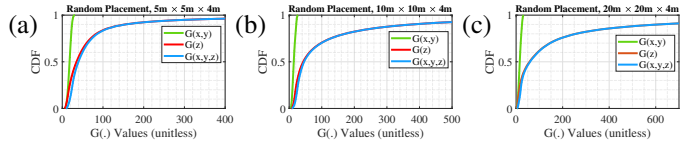

Figure 6: CDF plot representation of $G(.)$ values for various room dimensions with random configuration from Table II

results demonstrate that the algorithm consistently yields favorable outcomes across all tested scenarios.

Moreover, the figure underscores the significance of employing the proposed optimization algorithm for the deployment of 5G femtocells, as opposed to a random placement method. This preference is substantiated by the substantial influence of GDOP values on the overall accuracy of the system. In order to decrease the multiplicative factor in the $\sigma_T^2(x,y,z) = G(x,y,z) \cdot \sigma_r^2$, we want to attain lower GDOP values and by utilizing the proposed algorithm we achieved this goal.

In Fig. 5, the cumulative distribution function (CDF) of $G(.)$ values for optimal placement in three setups is depicted. This analysis aims to show the points in set $\mathbb{U}$ with $G(x,y,z)$ values below a specific threshold. The optimization objective was to ensure that most points had $G(x,y,z)$ values below 20, which is achieved in all scenarios, as shown in the figure.

For instance, in a typical office room, over 95% of $\mathbb{U}$ points have $G(x,y,z)$ values below 8, while in a large conference room, it's 14, and in a spacious game room, it's 12. These values, all below 20, confirm the effective performance of our optimization framework.

In order to establish a benchmark and emphasize the importance of optimal placement, we display in Figure 6 the same plots as in Figure 5, but with random placement. As seen in this figure, the $G(x,y,z)$ values rise to several hundred, rather than mostly staying below 20. This suggests that without the anchor placement strategy, the three-dimensional accuracy may be unreliable due to the high $G(x,y,z)$ values.

VI. Conclusion and Future Work

Conclusion. In this study, we focused on how the geometric relationship between a 5G-enabled Metaverse user and 5G femtocells impacts indoor localization accuracy. We found that errors result from both ranging and GDOP, where the latter is more affected by Z-axis estimation than $X-Y$ plane. To improve positioning accuracy, we developed an optimization algorithm for 5G femtocell placement. Our evaluations demonstrated that our approach notably enhances Z-axis estimation and overall GDOP, aligning with VDOP patterns.

Future Work. We have successfully established a 5G testbed utilizing OpenAirInterface (OAI) 5G within our controlled laboratory setting, and we have conducted comprehensive assessments encompassing resource utilization and over-the-air experiments [17]. Our future plans entail implementing the 5GPS system by integrating femtocells with this OAI 5G core, thereby creating a proof-of-concept demonstration.

References

[1] J. V.-V. Gerwen, K. Geebelen, J. Wan, W. Joseph, J. Hoebeke, and E. De Poorter, "Indoor drone positioning: Accuracy and cost trade-off for sensor fusion," *IEEE Transactions on Vehicular Technology*, vol. 71, no. 1, pp. 961–974, 2022.

[2] G. Chi, Z. Yang, J. Xu, C. Wu, J. Zhang, J. Liang, and Y. Liu, "Wi-Drone: Wi-Fi-based 6-DoF tracking for indoor drone flight control," in *Proceedings of the 20th Annual International Conference on Mobile Systems, Applications and Services*, ser. MobiSys '22. New York, NY, USA: Association for Computing Machinery, 2022, p. 56–68. [Online]. Available: https://doi.org/10.1145/3498361.3538936

[3] A. Famili, A. Stavrou, H. Wang, and J.-M. J. Park, "PILOT: high-precision indoor localization for autonomous drones," *IEEE Transactions on Vehicular Technology*, pp. 1–15, 2022.

[4] 3GPP, "NR; NR and NG-RAN Overall Description; Stage 2," 3rd Generation Partnership Project (3GPP), TS 38.300 V17.2.0, Sep. 2022.

[5] W. Wang, A. X. Liu, and K. Sun, "Device-free gesture tracking using acoustic signals," in *Proceedings of the 22nd Annual International Conference on Mobile Computing and Networking*, ser. MobiCom '16. New York, NY, USA: Association for Computing Machinery, 2016, p. 82–94. [Online]. Available: https://doi.org/10.1145/2973750.2973764

[6] A. Famili and J.-M. J. Park, "ROLATIN: robust localization and tracking for indoor navigation of drones," in *2020 IEEE Wireless Communications and Networking Conference (WCNC) (IEEE WCNC 2020)*, 2020.

[7] R. C. Luo and T.-J. Hsiao, "Indoor localization system based on hybrid Wi-Fi/BLE and hierarchical topological fingerprinting approach," *IEEE Transactions on Vehicular Technology*, pp. 10 791–10 806, 2019.

[8] G. Himona, A. Famili, A. Stavrou, V. Kovanis, and Y. Kominis, "Isochrons in tunable photonic oscillators and applications in precise positioning," in *Physics and Simulation of Optoelectronic Devices XXXI*, vol. 12415. SPIE, 2023, pp. 82–86.

[9] H. Wang, N. Rajagopal, A. Rowe, B. Sinopoli, and J. Gao, "Efficient beacon placement algorithms for time-of-flight indoor localization," in *Proceedings of the 27th ACM SIGSPATIAL International Conference on Advances in Geographic Information Systems*, ser. SIGSPATIAL '19. New York, NY, USA: Association for Computing Machinery, 2019, p. 119–128. [Online]. Available: https://doi.org/10.1145/3347146.3359344

[10] N. Rajagopal, S. Chayapathy, B. Sinopoli, and A. Rowe, "Beacon placement for range-based indoor localization," in *2016 International Conference on Indoor Positioning and Indoor Navigation (IPIN)*, Oct 2016, pp. 1–8.

[11] R. Sharma and V. Badarla, "Analysis of a novel beacon placement strategy 3D localization in indoor spaces," in *2019 11th International Conference on Communication Systems Networks (COMSNETS)*, Jan 2019, pp. 320–327.

[12] J. Schmalenstroeer and R. Haeb-Umbach, "Investigations into bluetooth low energy localization precision limits," in *2016 24th European Signal Processing Conference (EUSIPCO)*, Aug 2016, pp. 652–656.

[13] A. Famili, A. Stavrou, H. Wang, Jung-Min, and Park, "iDROP: Robust localization for indoor navigation of drones with optimized beacon placement," 2022.

[14] W. Dai, Y. Shen, and M. Z. Win, "A computational geometry framework for efficient network localization," *IEEE Transactions on Information Theory*, vol. 64, no. 2, pp. 1317–1339, 2018.

[15] T. Wang, Y. Shen, A. Conti, and M. Z. Win, "Network navigation with scheduling: Error evolution," *IEEE Transactions on Information Theory*, vol. 63, no. 11, pp. 7509–7534, 2017.

[16] A. Famili, A. Stavrou, H. Wang, and J.-M. Park, "SPIN: sensor placement for indoor navigation of drones," in *IEEE LATINCOM 2022*, nov 2022.

[17] T. O. Atalay, D. Stojadinovic, A. Famili, A. Stavrou, and H. Wang, "Network-Slice-as-a-Service Deployment Cost Assessment in an End-to-End 5G Testbed," in *2022 IEEE Global Communications Conference: Mobile and Wireless Networks (Globecom 2022 MWN)*, Dec. 2022.